Wigner distributions of sea quarks in the light-cone quark model

Xiaoyan Luan and Zhun Lu*

School of Physics, Southeast University, Nanjing 211189, China

(Received 31 January 2024; accepted 11 April 2024; published 10 May 2024)

We investigate the Wigner distributions of $\bar{u}$ and $\bar{d}$ quarks in a proton using the overlap representation within the light cone formalism. Using the light-cone wave functions which are obtained from the baryon-meson fluctuation model in terms of the $|q\bar{q}B\rangle$ Fock states, we calculate the Wigner distributions for the unpolarized/longitudinally polarized sea quarks in an unpolarized/longitudinally polarized proton. The Wigner distributions can be obtained through a Fourier transform on the generalized transverse-momentum dependent parton distributions (GTMDs). We also calculate the GTMDs of $\bar{u}$ and $\bar{d}$ quarks in the intermediate step. Numerical results for the Wigner distributions of $\bar{u}$ and $\bar{d}$ quarks in transverse momentum space, impact parameter space and the mixed plane are presented. We also study the orbital angular momentum and the spin-orbit correlations of the sea quarks.

DOI: 10.1103/PhysRevD.109.094016

I. INTRODUCTION

Understanding the internal structures of hadrons in terms of quarks and gluon is one of the main goals of QCD and hadronic physics. In order to describe the inclusive process with one hadron in the initial state, the parton distribution function (PDF) $f_{i/h}(x)$, which represents the probability density of parton i in a hadron h with the longitudinal momentum fraction x, was first introduced by Feynman [1]. Although very successful, PDFs can only describe partonic structure of hadrons in one dimension. In the last three decades, a much more comprehensive picture on the nucleon structure has been developed [2–6], and the transverse momentum dependent distributions (TMDs) play the central role. TMDs $f(x,\boldsymbol{k}_\perp)$ not only depend on the longitudinal momentum fraction x, but also depend on the parton transverse momentum $\boldsymbol{k}_\perp$ with respect to the hadron, therefore they allow a three-dimensional description of parton structure in momentum space. TMD distributions naturally enter the description of semi-inclusive deep inelastic scattering and Drell-Yan process in which two hadrons are involved.

Apart from TMDs, in the off-forward region a new type of nucleon structure—the so-called generalized parton distributions (GPDs) [7–15]—emerge. It is the extension of the ordinary PDF from the forward-scattering region to the off-forward scattering region. Therefore, GPDs are natural observables appearing in various exclusive processes in which the target receives a recoil momentum Δ, such as the deeply virtual Compton scattering (DVCS) $\gamma^* h(p) \to \gamma h(p')$ and the hard exclusive production of meson $\gamma^* h_1(p) \to M h_2(p')$. Except x, GPDs also depend on the momentum transfer squared $t = \Delta^2$ and the longitudinal fraction $\xi = \Delta^+/P^+$ of the transferred momentum. Particularly, Fourier transforming GPDs with respect to the transverse component of Δ yields the impact-parameter dependent distributions (IPDs) [16–18], $f(x, b_\perp^2)$, with $b_\perp$ the impact parameter conjugate to $\Delta_\perp$. IPDs thus provide useful information on the parton tomography in hadrons; distributions of parton in the transverse coordinate space at a fixed x.

A more fundamental understanding of the partonic structure of the nucleon can be gained by combining the distributions in momentum space and in position space. For this purpose, the Wigner distributions of quarks and gluons inside the nucleon [19,20] proposed and has been extensively studied in recent years. The original Wigner distributions for the nucleon are six-dimensional phase-space distributions, which provide a joint transverse momentum space (3D) and transverse position space (3D) about partons in the nucleon. Therefore, they encode far more information on the partonic structure of the nucleon than the standard parton distribution functions do. A very useful phase-space distribution for describing a fast moving hadron (or in the infinite-momentum frame) is the five-dimensional Wigner distribution [21], denoted by $W(x, k_\perp, b_\perp)$. On the one hand, the Wigner distributions reduce to the IPDs after integrating over transverse momenta. On the other hand, they reduce to TMDs after integrating over the transverse impact parameters. The Wigner distributions cannot be directly measured because

*zhunlu@seu.edu.cn

of the uncertainty principle which presents the position and momentum of a quantum-mechanical system cannot be simultaneously determined. Furthermore the Wigner distributions are usually recognized as quasidistribution functions which are in general not positive definite and have no probability interpretations. However, after integrating over several variables, a reduced Wigner distribution can become positive definite.

Through Fourier transform, the Wigner distributions are related to the generalized transverse momentum dependent parton distributions (GTMDs), which are often considered as the "mother distribution" for the TMDs and the GPDs [14,19,20]. GTMDs are functions of the light-cone momentum fraction, the transverse momentum of the parton as well as the transverse momentum transfer to the nucleon, and are obtained from the generalized parton correlation functions (GPCFs) [22,23] by integrating over the minus component of the parton momentum. Furthermore, the orbital angular momentum (OAM) of a parton as well as the spin-orbit correlations can be extracted from the Wigner distributions by taking the phase-space average [21,24,25].

In recent years, the Wigner distributions of the valence quarks [21,24–35] and gluon [36–39] in the nucleon have been studied in various models. In Refs. [21,26], the five-dimensional Wigner distributions $W(x, k_\perp, b_\perp)$ were calculated in the light-cone chiral-quark soliton model and the light-cone constituent quark model. Besides, the light-front dressed quark model [27,28,36], the spectator (diquark) model [29–31,31,32,32], the light-cone quark-diquark model [24,25] were applied to calculate the Wigner distribution of the proton. The light-cone quark model [34] was also used to calculate the Wigner distributions of the pion meson. However, the Wigner distribution of the sea quarks are less studied compared to those of the quarks and gluon.

In this paper, we apply the light-cone quark model to calculate the five-dimensional Wigner distributions $\rho(x, \boldsymbol{b}_T, \boldsymbol{k}_T)$ of the $\bar{u}$ and $\bar{d}$ quarks. As pointed out in Ref. [21], the light-cone formalism is a suitable approach for studying Wigner distributions, since in leading twist the Wigner distributions can be expressed as the overlap integration of hadronic light-cone wave functions [40]. To generate the sea quark degree freedom, we applied the meson-baryon fluctuation model proposed in Refs. [41]. In this model, the proton has the possibility to fluctuate into a composite state with a meson M and a baryon B, and consequently the meson M contains the $q\bar{q}$ Fock states. The light-cone wave functions (LCWFs) of the proton thus may be derived in terms of the $|q\bar{q}B\rangle$ Fock states, as calculated in Ref. [42]. The expressions of the Wigner distributions of the unpolarized/longitudinally polarized sea quarks in an unpolarized/longitudinally polarized proton (ρ_{UU}, ρ_{LU}, ρ_{LL}, ρ_{UL}) can be obtained in the general case within the overlap representation. The numerical results of these Wigner distributions are calculated using the LCWFs from the meson-baryon fluctuation model. In the intermediate calculation, the expression of the $\bar{u}$ and $\bar{d}$ quarks GTMD are obtained. We also study the OAM and the spin-orbit correlations of $\bar{u}$ and $\bar{d}$ quarks using the relation between the Wigner distributions and GTMDs.

The remained part of the paper is organized as follows. In Sec. II, we introduce the definition of the Wigner distributions and their connection with GTMDs. In Sec. III, we apply the overlap representation to obtain the expressions of the Wigner distributions and GTMDs of the sea quarks. In Sec. VI, we present the numerical results of the unpolarized and longitudinally polarized Wigner distributions in the transverse position space, transverse momentum space and mixed space. We summarize the paper in Sec. V.

II. WIGNER DISTRIBUTIONS AND GTMDS

The Wigner distribution of partons inside a hadron can be defined as the two-dimensional Fourier transforms of the GTMDs. In the light-front framework, the five-dimensional Wigner distribution is written as [21,23]

$$\rho^{[\Gamma]}_{\Lambda'\Lambda}(x, \boldsymbol{b}_T, \boldsymbol{k}_T) = \int \frac{\mathrm{d}^2\boldsymbol{\Delta}_T}{(2\pi)^2} e^{-i\boldsymbol{\Delta}_T\cdot \boldsymbol{b}_T} W^{[\Gamma]}_{\Lambda'\Lambda}(x, \boldsymbol{\Delta}_T, \boldsymbol{k}_T), \tag{1}$$

where $\boldsymbol{\Delta}_T$ is the momentum transfer from the initial state to the final state in the transverse direction, and $\boldsymbol{b}_T$ is the impact parameter in the position space conjugate to $\boldsymbol{\Delta}_T$. Similar to the standard quark-quark correlation operator, the generalized correlator $W^{[\Gamma]}_{\Lambda'\Lambda}(x, \boldsymbol{\Delta}_T, \boldsymbol{k}_T)$ at $\xi = 0$ and a fixed light-cone time is defined as

$$W^{[\Gamma]}_{\Lambda'\Lambda}(x, \boldsymbol{\Delta}_T, \boldsymbol{k}_T) = \int \frac{dz^- d^2z_T}{2(2\pi)^3} e^{ik\cdot z} \langle p'\Lambda'|\bar{\psi}\left(-\frac{z}{2}\right)\Gamma\mathcal{W}\psi\left(\frac{z}{2}\right)|p\Lambda\rangle\Big|_{z^+=0}, \tag{2}$$

where $\mathcal{W}$ is the gauge link connecting the quark fields at positions $-\frac{z}{2}$ and $\frac{z}{2}$ to ensure the color gauge invariance, $p\Lambda$ ($p'\Lambda'$) are the momenta and helicities of the initial (final) state nucleon, $P = (p + p')/2$ is the average four-momentum of the nucleon, $x = k^+/P^+$ is the average fraction of the light-cone momentum carried by the active quark, Γ represents the Dirac matrix structure. In this work we take $\Gamma = \gamma^+, \gamma^+\gamma^5$.

The generalized correlator in Eq. (2) can be parametrized in terms of GTMDs [23]. At leading twist $\Gamma = \gamma^+$ or $\gamma^+\gamma^5$, we have eight GTMDs defined as follows:

$$W_{\Lambda'\Lambda}^{[\gamma^+]} = \frac{1}{2M}\bar{U}(p',\Lambda')\left[F_{11} + \frac{i\sigma^{i+}k^i}{P^+}F_{12} + \frac{i\sigma^{i+}\Delta^i}{P^+}F_{13} + \frac{i\sigma^{ij}k^i\Delta^j}{M^2}F_{14}\right]U(p,\Lambda)$$
$$= \left[F_{11} + \frac{i\Lambda\epsilon^{ij}k^i\Delta^j}{M^2}F_{14}\right]\delta_{\Lambda'\Lambda} + \left[\frac{\Lambda\Delta^1 + i\Delta^2}{2M}(2F_{13} - F_{11}) + \frac{\Lambda k^1 + ik^2}{M}F_{12}\right]\delta_{-\Lambda'\Lambda}, \tag{3}$$

$$W_{\Lambda'\Lambda}^{[\gamma^+\gamma^5]} = \frac{1}{2M}\bar{U}(p',\Lambda')\left[-\frac{i\epsilon^{ij}k^i\Delta^j}{M^2}G_{11} + \frac{i\sigma^{i+}\gamma^5k^i}{P^+}G_{12} + \frac{i\sigma^{i+}\gamma^5\Delta^i}{P^+}G_{13} + i\sigma^{+-}\gamma^5G_{14}\right]U(p,\Lambda)$$
$$= \left[-\frac{i(k^1\Delta^2 - k^2\Delta^1)}{M^2}G_{11} + \Lambda G_{14}\right]\delta_{\Lambda'\Lambda} + \left[\frac{\Delta^1 + i\Lambda\Delta^2}{M}\left(G_{13} + \frac{i\Lambda(k^1\Delta^2 - k^2\Delta^1)}{2M^2}G_{11}\right) + \frac{k^1 + i\Lambda k^2}{M}G_{12}\right]\delta_{-\Lambda'\Lambda}. \tag{4}$$

where $\epsilon^{ij} = \epsilon^{-+ij}$ and $\epsilon^{0123} = 1$. The GTMDs F_{11}, F_{12}, F_{13}, F_{14}, in Eq. (3) describe the distribution for the unpolarized quark, while the GTMDs G_{11}, G_{12}, G_{13}, G_{14}, in Eq. (4) describe those for the longitudinally polarized quark. They are considered to be complex functions of the kinematical variables $x, \xi, \boldsymbol{\Delta}_T^2, \boldsymbol{k}_T \cdot \boldsymbol{\Delta}_T, \boldsymbol{k}_T^2$.

Using + (−) to denote the positive (negative) helicity of the proton, we can obtain the following expressions for the terms in which the proton helicity is not flipped [43],

$$F_{11}(x,\boldsymbol{\Delta}_T,\boldsymbol{k}_T) = \frac{1}{2}[W_{++}^{[\gamma^+]}(x,\boldsymbol{\Delta}_T,\boldsymbol{k}_T) + W_{--}^{[\gamma^+]}(x,\boldsymbol{\Delta}_T,\boldsymbol{k}_T)], \tag{5}$$

$$i\frac{\boldsymbol{k}_T \times \boldsymbol{\Delta}_T}{M^2}F_{14}(x,\boldsymbol{\Delta}_T,\boldsymbol{k}_T) = \frac{1}{2}[W_{++}^{[\gamma^+]}(x,\boldsymbol{\Delta}_T,\boldsymbol{k}_T) - W_{--}^{[\gamma^+]}(x,\boldsymbol{\Delta}_T,\boldsymbol{k}_T)], \tag{6}$$

$$-i\frac{\boldsymbol{k}_T \times \boldsymbol{\Delta}_T}{M^2}G_{11}(x,\boldsymbol{\Delta}_T,\boldsymbol{k}_T) = \frac{1}{2}[W_{++}^{[\gamma^+\gamma^5]}(x,\boldsymbol{\Delta}_T,\boldsymbol{k}_T) + W_{--}^{[\gamma^+\gamma^5]}(x,\boldsymbol{\Delta}_T,\boldsymbol{k}_T)], \tag{7}$$

$$G_{14}(x,\boldsymbol{\Delta}_T,\boldsymbol{k}_T) = \frac{1}{2}[W_{++}^{[\gamma^+\gamma^5]}(x,\boldsymbol{\Delta}_T,\boldsymbol{k}_T) - W_{--}^{[\gamma^+\gamma^5]}(x,\boldsymbol{\Delta}_T,\boldsymbol{k}_T)], \tag{8}$$

and expressions for the helicity-flipped terms [43],

$$-i\frac{\boldsymbol{k}_T \times \boldsymbol{\Delta}_T}{M}F_{12} = \frac{1}{2}[((\Delta^1 - i\Delta^2)W_{-+}^{[\gamma^+]} + (\Delta^1 + i\Delta^2)W_{+-}^{[\gamma^+]}], \tag{9}$$

$$\frac{\boldsymbol{k}_T \cdot \boldsymbol{\Delta}_T}{M}F_{12} + \frac{\boldsymbol{\Delta}_T^2}{2M}(2F_{13} - F_{11}) = \frac{1}{2}[((\Delta^1 - i\Delta^2)W_{-+}^{[\gamma^+]} - (\Delta^1 + i\Delta^2)W_{+-}^{[\gamma^+]}], \tag{10}$$

$$\frac{\boldsymbol{\Delta}_T^2}{M}G_{13} + \frac{\boldsymbol{k}_T \cdot \boldsymbol{\Delta}_T}{M}G_{12} = \frac{1}{2}[((\Delta^1 - i\Delta^2)W_{-+}^{[\gamma^+\gamma^5]} + (\Delta^1 + i\Delta^2)W_{+-}^{[\gamma^+\gamma^5]}], \tag{11}$$

$$\frac{i(\boldsymbol{k}_T \times \boldsymbol{\Delta}_T)}{M}\left(\frac{\boldsymbol{\Delta}_T^2}{2M^2}G_{11} - G_{12}\right) = \frac{1}{2}[(\Delta^1 - i\Delta^2)W_{-+}^{[\gamma^+\gamma^5]} - (\Delta^1 + i\Delta^2)W_{+-}^{[\gamma^+\gamma^5]}]. \tag{12}$$

Using the notation in Eq. (1), one can define four Wigner distributions. The first one is the Wigner distribution of the unpolarized quark in the unpolarized target,

$$\rho_{UU}(x,\boldsymbol{b}_T,\boldsymbol{k}_T) = \frac{1}{2}[\rho_{++}^{[\gamma^+]}(x,\boldsymbol{b}_T,\boldsymbol{k}_T) + \rho_{--}^{[\gamma^+]}(x,\boldsymbol{b}_T,\boldsymbol{k}_T)], \tag{13}$$

the second one is the Wigner distribution of the unpolarized quark in the longitudinally polarized target,

$$\rho_{LU}(x,\boldsymbol{b}_T,\boldsymbol{k}_T) = \frac{1}{2}[\rho_{++}^{[\gamma^+]}(x,\boldsymbol{b}_T,\boldsymbol{k}_T) - \rho_{--}^{[\gamma^+]}(x,\boldsymbol{b}_T,\boldsymbol{k}_T)], \tag{14}$$

the third one is the Wigner distribution of the longitudinally polarized quark in the unpolarized target,

$$\rho_{UL}(x,\boldsymbol{b}_T,\boldsymbol{k}_T) = \frac{1}{2}[\rho_{++}^{[\gamma^+\gamma^5]}(x,\boldsymbol{b}_T,\boldsymbol{k}_T) + \rho_{--}^{[\gamma^+\gamma^5]}(x,\boldsymbol{b}_T,\boldsymbol{k}_T)], \tag{15}$$

and the last one is the Wigner distribution of the longitudinally polarized quark in the longitudinally polarized target

$$\rho_{LL}(x,\boldsymbol{b}_T,\boldsymbol{k}_T)=\frac{1}{2}[\rho_{++}^{[\gamma^+\gamma^5]}(x,\boldsymbol{b}_T,\boldsymbol{k}_T)-\rho_{--}^{[\gamma^+\gamma^5]}(x,\boldsymbol{b}_T,\boldsymbol{k}_T)]. \tag{16}$$

Finally, these Wigner distributions can be obtained from the GTMDs,

$$\rho_{UU}(x,\boldsymbol{b}_T,\boldsymbol{k}_T)=\mathcal{F}_{11}(x,0,\boldsymbol{k}_T^2,\boldsymbol{k}_T\cdot\boldsymbol{b}_T,\boldsymbol{b}_T^2), \tag{17}$$

$$\rho_{LU}(x,\boldsymbol{b}_T,\boldsymbol{k}_T)=-\frac{1}{M^2}\epsilon_T^{ij}k_T^i\frac{\partial}{\partial b_T^j}\mathcal{F}_{14}(x,0,\boldsymbol{k}_T^2,\boldsymbol{k}_T\cdot\boldsymbol{b}_T,\boldsymbol{b}_T^2), \tag{18}$$

$$\rho_{UL}(x,\boldsymbol{b}_T,\boldsymbol{k}_T)=\frac{1}{M^2}\epsilon_T^{ij}k_T^i\frac{\partial}{\partial b_T^j}\mathcal{G}_{11}(x,0,\boldsymbol{k}_T^2,\boldsymbol{k}_T\cdot\boldsymbol{b}_T,\boldsymbol{b}_T^2), \tag{19}$$

$$\rho_{LL}(x,\boldsymbol{b}_T,\boldsymbol{k}_T)=\mathcal{G}_{14}(x,0,\boldsymbol{k}_T^2,\boldsymbol{k}_T\cdot\boldsymbol{b}_T,\boldsymbol{b}_T^2), \tag{20}$$

where $\mathcal{X}$ is the Fourier transform of the corresponding GTMD X,

$$\mathcal{X}(x,\boldsymbol{b}_T,\boldsymbol{k}_T)=\int\frac{\mathrm{d}^2\boldsymbol{\Delta}_T}{(2\pi)^2}e^{-i\boldsymbol{\Delta}_T\cdot\boldsymbol{b}_T}X(x,\boldsymbol{\Delta}_T,\boldsymbol{k}_T). \tag{21}$$

III. SEA QUARK WIGNER DISTRIBUTIONS OF THE PROTON IN THE OVERLAP REPRESENTATION

In this section we present the calculation on the sea quark Wigner distributions of the proton in the light-cone model using the overlap representation. The light-cone formalism has been widely recognized as a convenient way to calculate the parton distribution functions of nucleon and meson [44]. Within the light-cone approach, a hadronic composite state can be expressed as LCWFs on the Fock-state basis. The overlap representation has also been used to study various form factors of the hadrons [45,46], anomalous magnetic moment of the nucleon [45], TMDs [47,48] as well as GPDs [32,49–51]. Recently, the overlap representation of LCWFs has also been applied to calculate the quark Wigner distributions [34,52]. Here we extend light-cone formalism to calculate the Wigner distributions and GTMDs of the sea quarks.

The baryon-meson fluctuation model [41] is adopted to generate the degree of freedom of sea quark, in which the proton can fluctuate to a composite system formed by a meson M and a baryon B, where the meson is composed in terms of $q\bar{q}$,

$$|p\rangle\to|MB\rangle\to|q\bar{q}B\rangle. \tag{22}$$

In our work, we consider the fluctuation $|p\rangle\to|\pi^+n\rangle$ and $|p\rangle\to|\pi^-\Delta^{++}\rangle$. The corresponding LCWFs have the form which have been derived in Ref. [42],

$$\psi^{\lambda_N}_{\lambda_B\lambda_q\lambda_{\bar{q}}}(x,y,\boldsymbol{k}_T,\boldsymbol{r}_T)=\psi^{\lambda_N}_{\lambda_B}(y,\boldsymbol{r}_T)\psi_{\lambda_q\lambda_{\bar{q}}}(x,y,\boldsymbol{k}_T,\boldsymbol{r}_T), \tag{23}$$

where $\psi^{\lambda_N}_{\lambda_B}(y,r_T)$ can be viewed as the wave function of the nucleon in terms πB components, and $\psi_{\lambda_q\lambda_{\bar{q}}}(x,y,\boldsymbol{k}_T,\boldsymbol{r}_T)$ is the pion wave function in terms of $q\bar{q}$ components. The indices λ_N, λ_B, λ_q, $\lambda_{\bar{q}}$, denote the helicity of the proton, the baryon, the quark and the sea quark, respectively. x and y represent their light-cone momentum fractions, $\boldsymbol{k}_T$ and $\boldsymbol{r}_T$ denote the transverse momenta of the antiquark and the meson. For the former one of Eq. (23), they have the expression,

$$\begin{aligned}
\psi^+_+(y,\boldsymbol{r}_T)&=\frac{M_B-(1-y)M}{\sqrt{1-y}}\phi_1,\\
\psi^+_-(y,\boldsymbol{r}_T)&=\frac{r_1+ir_2}{\sqrt{1-y}}\phi_1,\\
\psi^-_+(y,\boldsymbol{r}_T)&=\frac{r_1-ir_2}{\sqrt{1-y}}\phi_1,\\
\psi^-_-(y,\boldsymbol{r}_T)&=\frac{(1-y)M-M_B}{\sqrt{1-y}}\phi_1,
\end{aligned} \tag{24}$$

Here, M and M_B are the masses of proton and baryon, respectively. ϕ_1 is the momentum space wave function of the bayron-meson Fock state,

$$\phi_1(y,\boldsymbol{r}_T)=-\frac{g(r^2)\sqrt{y(1-y)}}{\boldsymbol{r}_T^2+L_1^2(m_\pi^2)}, \tag{25}$$

where m_π is the mass of π meson, $g(r^2)$ is the form factor for the coupling of the nucleon-pion meson-baryon vertex, and

$$L_1^2(m_\pi^2)=yM_B^2+(1-y)m_\pi^2-y(1-y)M^2. \tag{26}$$

The latter one of Eq. (23) have the following expressions:

$$\begin{aligned}
\psi_{++}(x,y,\boldsymbol{k}_T,\boldsymbol{r}_T)&=\frac{my}{\sqrt{x(y-x)}}\phi_2,\\
\psi_{+-}(x,y,\boldsymbol{k}_T,\boldsymbol{r}_T)&=\frac{y(k_1-ik_2)-x(r_1-ir_2)}{\sqrt{x(y-x)}}\phi_2,\\
\psi_{-+}(x,y,\boldsymbol{k}_T,\boldsymbol{r}_T)&=\frac{y(k_1+ik_2)-x(r_1+ir_2)}{\sqrt{x(y-x)}}\phi_2,\\
\psi_{--}(x,y,\boldsymbol{k}_T,\boldsymbol{r}_T)&=\frac{-my}{\sqrt{x(y-x)}}\phi_2,
\end{aligned} \tag{27}$$

where m is the mass of quark and the sea quark. Again, $\phi_2(x, y, \boldsymbol{k}_T, \boldsymbol{r}_T)$ is the momentum space wave function of the $|q\bar{q}\rangle$ Fock state,

$$\phi_2(x, y, \boldsymbol{k}_T, \boldsymbol{r}_T) = -\frac{g(k^2)\sqrt{\frac{x}{y}(1-\frac{x}{y})}}{(\boldsymbol{k}_T - \frac{x}{y}\boldsymbol{r}_T)^2 + L_2^2(m^2)}, \quad (28)$$

$g(k^2)$ is the form factor for the coupling of the pion meson-quark sea-quark vertex, and

$$L_2^2(m^2) = \frac{x}{y}m^2 + \left(1-\frac{x}{y}\right)m^2 - \frac{x}{y}\left(1-\frac{x}{y}\right)m_\pi{}^2. \quad (29)$$

For the form factors $g(r^2)$ and $g(k^2)$, we adopt the dipolar form,

$$g(r^2) = -g_1(1-y)\frac{\boldsymbol{r}_T^2 + L_1^2(m_\pi^2)}{[\boldsymbol{r}_T^2 + L_1^2(\Lambda_\pi^2)]^2}, \quad (30)$$

$$g(k^2) = -g_2\left(1-\frac{x}{y}\right)\frac{(\boldsymbol{k}_T - \frac{x}{y}\boldsymbol{r}_T)^2 + L_2^2(m^2)}{[(\boldsymbol{k}_T - \frac{x}{y}\boldsymbol{r}_T)^2 + L_2^2(\Lambda_{\bar{q}}^2)]^2}. \quad (31)$$

In the overlap representation, the leading-twist generalized correlator can be expressed as

$$W^{[\gamma^+]}_{\Lambda'\Lambda}(x, \boldsymbol{k}_T, \boldsymbol{\Delta}_T) = \int\frac{d^2\boldsymbol{r}_T}{16\pi^3}\int_x^1\frac{dy}{y} \times\sum_{\{\lambda\}}(\psi^{\Lambda'\star}_{\lambda_B\lambda_q\lambda_{\bar{q}}}(x^{\rm out}, y^{\rm out}, \boldsymbol{k}_T^{\rm out}, \boldsymbol{r}_T^{\rm out}) \times\psi^{\Lambda}_{\lambda_B\lambda_q\lambda_{\bar{q}}}(x^{\rm in}, y^{\rm in}, \boldsymbol{k}_T^{\rm in}, \boldsymbol{r}_T^{\rm in})), \quad (32)$$

$$W^{[\gamma^+\gamma^5]}_{\Lambda'\Lambda}(x, \boldsymbol{k}_T, \boldsymbol{\Delta}_T) = \int\frac{d^2\boldsymbol{r}_T}{16\pi^3}\int_x^1\frac{dy}{y}\,\mathrm{sign}(\lambda_{\bar{q}}) \times\sum_{\{\lambda\}}(\psi^{\Lambda'\star}_{\lambda_B\lambda_q\lambda_{\bar{q}}}(x^{\rm out}, y^{\rm out}, \boldsymbol{k}_T^{\rm out}, \boldsymbol{r}_T^{\rm out}) \times\psi^{\Lambda}_{\lambda_B\lambda_q\lambda_{\bar{q}}}(x^{\rm in}, y^{\rm in}, \boldsymbol{k}_T^{\rm in}, \boldsymbol{r}_T^{\rm in})). \quad (33)$$

where $\{\lambda\} = \lambda_B, \lambda_q, \lambda_{\bar{q}}$. The momentum fractions for the final-state and initial-state antiquark $\bar{q}$ and the meson can be expressed as

$$x^{\rm out} = \frac{x-\xi}{1-\xi}, \qquad x^{\rm in} = \frac{x+\xi}{1+\xi},$$
$$y^{\rm out} = \frac{y-\xi}{1-\xi}, \qquad y^{\rm in} = \frac{y+\xi}{1+\xi}, \quad (34)$$

and

$$\boldsymbol{k}_T^{\rm out} = \boldsymbol{k}_T - \frac{1}{2}(1-x^{\rm out})\boldsymbol{\Delta}_T,$$
$$\boldsymbol{k}_T^{\rm in} = \boldsymbol{k}_T + \frac{1}{2}(1-x^{\rm in})\boldsymbol{\Delta}_T, \quad (35)$$

are the expressions for transverse momenta for the antiquark. Finally, the transverse momenta for the spectator baryon and the quark has the form,

$$-\boldsymbol{r}_T^{\rm out} = -\boldsymbol{r}_T + \frac{1}{2}(1-y)\boldsymbol{\Delta}_T,$$
$$-\boldsymbol{r}_T^{\rm in} = -\boldsymbol{r}_T - \frac{1}{2}(1-y)\boldsymbol{\Delta}_T,$$
$$(\boldsymbol{r}_T - \boldsymbol{k}_T)^{\rm out} = (\boldsymbol{r}_T - \boldsymbol{k}_T) + \frac{1}{2}(y-x)\boldsymbol{\Delta}_T,$$
$$(\boldsymbol{r}_T - \boldsymbol{k}_T)^{\rm in} = (\boldsymbol{r}_T - \boldsymbol{k}_T) - \frac{1}{2}(y-x)\boldsymbol{\Delta}_T. \quad (36)$$

Using the LCWFs in Eqs. (24)–(27) and the overlap representation for the generalized correlator in Eqs. (32)–(33), we get the results of the GTMDs of the sea quark in proton at $\xi = 0$,

$$F_{11}(x, \boldsymbol{\Delta}_T, \boldsymbol{k}_T) = \frac{g_1^2 g_2^2}{8\pi^3}\int_x^1\frac{dy}{y}\int d^2\boldsymbol{r}_T \times\frac{y(1-y)^2(1-\frac{x}{y})^2[\boldsymbol{r}_T^2 - \frac{1}{4}(1-y)^2\boldsymbol{\Delta}_T^2 + [M_B-(1-y)M]^2][(\boldsymbol{k}_T - \frac{x}{y}\boldsymbol{r}_T)^2 - \frac{1}{4}(1-\frac{x}{y})^2\boldsymbol{\Delta}_T^2 + m^2]}{D_1(y, \boldsymbol{r}_T, \boldsymbol{\Delta}_T)D_2(\frac{x}{y}, \boldsymbol{k}_T - \frac{x}{y}\boldsymbol{r}_T, \boldsymbol{\Delta}_T)}, \quad (37)$$

$$F_{12}(x, \boldsymbol{\Delta}_T, \boldsymbol{k}_T) = 0, \quad (38)$$

$$F_{13}(x, \boldsymbol{\Delta}_T, \boldsymbol{k}_T) = \frac{g_1^2 g_2^2}{16\pi^3}\int_x^1\frac{dy}{y}\int d^2\boldsymbol{r}_T y(1-y)^2\left(1-\frac{x}{y}\right)^2\frac{[(\boldsymbol{k}_T - \frac{x}{y}\boldsymbol{r}_T)^2 - \frac{1}{4}(1-\frac{x}{y})^2\boldsymbol{\Delta}_T^2 + m^2]}{D_2(\frac{x}{y}, \boldsymbol{k}_T - \frac{x}{y}\boldsymbol{r}_T, \boldsymbol{\Delta}_T)} \times\frac{[2M(1-y)[(1-y)M - M_B] + \boldsymbol{r}_T^2 - \frac{1}{4}(1-y)^2\boldsymbol{\Delta}_T^2 + [M_B-(1-y)M]^2]}{D_1(y, \boldsymbol{r}_T, \boldsymbol{\Delta}_T)}, \quad (39)$$

$$F_{14}(x,\mathbf{\Delta}_T,\boldsymbol{k}_T)=\frac{g_1^2g_2^2}{8\pi^3}\int_x^1\frac{dy}{y}\int d^2\boldsymbol{r}_T\frac{y(1-y)^3(1-\frac{x}{y})^2M^2[(\boldsymbol{k}_T-\frac{x}{y}\boldsymbol{r}_T)^2-\frac{1}{4}(1-\frac{x}{y})^2\mathbf{\Delta}_T^2+m^2]}{D_1(y,\boldsymbol{r}_T,\mathbf{\Delta}_T)D_2(\frac{x}{y},\boldsymbol{k}_T-\frac{x}{y}\boldsymbol{r}_T,\mathbf{\Delta}_T)}\cdot\frac{\boldsymbol{r}_T\times\mathbf{\Delta}_T}{\boldsymbol{k}_T\times\mathbf{\Delta}_T},$$

$$G_{11}(x,\mathbf{\Delta}_T,\boldsymbol{k}_T)=-\frac{g_1^2g_2^2}{8\pi^3}\int_x^1\frac{dy}{y}\int d^2\boldsymbol{r}_T \times\frac{y(1-y)^2(1-\frac{x}{y})^3M^2[\boldsymbol{r}_T^2-\frac{1}{4}(1-y)^2\mathbf{\Delta}_T^2+[M_B-(1-y)M]^2]}{D_1(y,\boldsymbol{r}_T,\mathbf{\Delta}_T)D_2(\frac{x}{y},\boldsymbol{k}_T-\frac{x}{y}\boldsymbol{r}_T,\mathbf{\Delta}_T)}\cdot\frac{(\boldsymbol{k}_T-\frac{x}{y}\boldsymbol{r}_T)\times\mathbf{\Delta}_T}{\boldsymbol{k}_T\times\mathbf{\Delta}_T},\qquad(40)$$

$$G_{12}(x,\mathbf{\Delta}_T,\boldsymbol{k}_T)=\frac{g_1^2g_2^2}{16\pi^3}\int_x^1\frac{dy}{y}\int d^2\boldsymbol{r}_T y(1-y)^2\left(1-\frac{x}{y}\right)^3 \times\frac{\mathbf{\Delta}_T^2[2M(1-y)(M_B-(1-y)M)-\boldsymbol{r}_T^2+\frac{1}{4}(1-y)^2\mathbf{\Delta}_T^2-[M_B-(1-y)M]^2]}{D_1(y,\boldsymbol{r}_T,\mathbf{\Delta}_T)D_2(\frac{x}{y},\boldsymbol{k}_T-\frac{x}{y}\boldsymbol{r}_T,\mathbf{\Delta}_T)}\cdot\frac{(\boldsymbol{k}_T-\frac{x}{y}\boldsymbol{r}_T)\times\mathbf{\Delta}_T}{\boldsymbol{k}_T\times\mathbf{\Delta}_T},\qquad(41)$$

$$G_{13}(x,\mathbf{\Delta}_T,\boldsymbol{k}_T)=-\frac{g_1^2g_2^2}{16\pi^3}\int_x^1\frac{dy}{y}\int d^2\boldsymbol{r}_T y(1-y)^2\left(1-\frac{x}{y}\right)^3 \times\frac{\boldsymbol{k}_T\cdot\mathbf{\Delta}_T[2M(1-y)(M_B-(1-y)M)-\boldsymbol{r}_T^2+\frac{1}{4}(1-y)^2\mathbf{\Delta}_T^2-[M_B-(1-y)M]^2]}{D_1(y,\boldsymbol{r}_T,\mathbf{\Delta}_T)D_2(\frac{x}{y},\boldsymbol{k}_T-\frac{x}{y}\boldsymbol{r}_T,\mathbf{\Delta}_T)}\cdot\frac{(\boldsymbol{k}_T-\frac{x}{y}\boldsymbol{r}_T)\times\mathbf{\Delta}_T}{\boldsymbol{k}_T\times\mathbf{\Delta}_T},\qquad(42)$$

$$G_{14}(x,\mathbf{\Delta}_T,\boldsymbol{k}_T)=-\frac{g_1^2g_2^2}{8\pi^3}\int_x^1\frac{dy}{y}\int d^2\boldsymbol{r}_T\frac{y(1-y)^3(1-\frac{x}{y})^2\cdot\boldsymbol{r}_T\times\mathbf{\Delta}_T\cdot(\boldsymbol{k}_T-\frac{x}{y}\boldsymbol{r}_T)\times\mathbf{\Delta}_T}{D_1(y,\boldsymbol{r}_T,\mathbf{\Delta}_T)D_2(\frac{x}{y},\boldsymbol{k}_T-\frac{x}{y}\boldsymbol{r}_T,\mathbf{\Delta}_T)},\qquad(43)$$

where

$$D_1(y,\boldsymbol{r}_T,\mathbf{\Delta}_T)=\left[\left(\boldsymbol{r}_T-\frac{1}{2}(1-y)\mathbf{\Delta}_T\right)^2+L_1^2\right]^2\left[\left(\boldsymbol{r}_T+\frac{1}{2}(1-y)\mathbf{\Delta}_T\right)^2+L_1^2\right]^2,$$
$$D_2\left(\frac{x}{y},\boldsymbol{k}_T-\frac{x}{y}\boldsymbol{r}_T,\mathbf{\Delta}_T\right)=\left[\left[\left(\boldsymbol{k}_T-\frac{x}{y}\boldsymbol{r}_T\right)-\frac{1}{2}\left(1-\frac{x}{y}\right)\mathbf{\Delta}_T\right]^2+L_2^2\right]^2\left[\left[\left(\boldsymbol{k}_T-\frac{x}{y}\boldsymbol{r}_T\right)+\frac{1}{2}\left(1-\frac{x}{y}\right)\mathbf{\Delta}_T\right]^2+L_2^2\right]^2.\qquad(44)$$

Similarly, the Wigner distributions for unpolarized/longitudinally polarized sea quarks in an unpolarized/longitudinally polarized proton can be also calculated from the proton LCWFs within the overlap representation,

$$\rho_{UU}^{\bar{q}/P}=\frac{1}{2}\int\frac{d^2\boldsymbol{r}_T}{16\pi^3}\int_x^1\frac{dy}{y}\int\frac{\mathrm{d}^2\mathbf{\Delta}_T}{(2\pi)^2}e^{-i\mathbf{\Delta}_T\cdot\boldsymbol{b}_T}\sum_{\{\lambda\}}(\psi^{+\star}_{\lambda_B\lambda_q\lambda_{\bar{q}}}(x^{\rm out},y^{\rm out},\boldsymbol{k}_T^{\rm out},\boldsymbol{r}_T^{\rm out})\psi^{+}_{\lambda_B\lambda_q\lambda_{\bar{q}}}(x^{\rm in},y^{\rm in},\boldsymbol{k}_T^{\rm in},\boldsymbol{r}_T^{\rm in}) +\psi^{-\star}_{\lambda_B\lambda_q\lambda_{\bar{q}}}(x^{\rm out},y^{\rm out},\boldsymbol{k}_T^{\rm out},\boldsymbol{r}_T^{\rm out})\psi^{-}_{\lambda_B\lambda_q\lambda_{\bar{q}}}(x^{\rm in},y^{\rm in},\boldsymbol{k}_T^{\rm in},\boldsymbol{r}_T^{\rm in})),\qquad(45)$$

$$\rho_{LU}^{\bar{q}/P}=\frac{1}{2}\int\frac{d^2\boldsymbol{r}_T}{16\pi^3}\int_x^1\frac{dy}{y}\int\frac{\mathrm{d}^2\mathbf{\Delta}_T}{(2\pi)^2}e^{-i\mathbf{\Delta}_T\cdot\boldsymbol{b}_T}\sum_{\{\lambda\}}(\psi^{+\star}_{\lambda_B\lambda_q\lambda_{\bar{q}}}(x^{\rm out},y^{\rm out},\boldsymbol{k}_T^{\rm out},\boldsymbol{r}_T^{\rm out})\psi^{+}_{\lambda_B\lambda_q\lambda_{\bar{q}}}(x^{\rm in},y^{\rm in},\boldsymbol{k}_T^{\rm in},\boldsymbol{r}_T^{\rm in}) -\psi^{-\star}_{\lambda_B\lambda_q\lambda_{\bar{q}}}(x^{\rm out},y^{\rm out},\boldsymbol{k}_T^{\rm out},\boldsymbol{r}_T^{\rm out})\psi^{-}_{\lambda_B\lambda_q\lambda_{\bar{q}}}(x^{\rm in},y^{\rm in},\boldsymbol{k}_T^{\rm in},\boldsymbol{r}_T^{\rm in})),\qquad(46)$$

$$\rho_{UL}^{\bar{q}/P}=\frac{1}{2}\int\frac{d^2\boldsymbol{r}_T}{16\pi^3}\int_x^1\frac{dy}{y}\int\frac{\mathrm{d}^2\mathbf{\Delta}_T}{(2\pi)^2}e^{-i\mathbf{\Delta}_T\cdot\boldsymbol{b}_T}\mathrm{sign}(\lambda_{\bar{q}})\sum_{\{\lambda\}}(\psi^{+\star}_{\lambda_B\lambda_q\lambda_{\bar{q}}}(x^{\rm out},y^{\rm out},\boldsymbol{k}_T^{\rm out},\boldsymbol{r}_T^{\rm out})\psi^{+}_{\lambda_B\lambda_q\lambda_{\bar{q}}}(x^{\rm in},y^{\rm in},\boldsymbol{k}_T^{\rm in},\boldsymbol{r}_T^{\rm in}) +\psi^{-\star}_{\lambda_B\lambda_q\lambda_{\bar{q}}}(x^{\rm out},y^{\rm out},\boldsymbol{k}_T^{\rm out},\boldsymbol{r}_T^{\rm out})\psi^{-}_{\lambda_B\lambda_q\lambda_{\bar{q}}}(x^{\rm in},y^{\rm in},\boldsymbol{k}_T^{\rm in},\boldsymbol{r}_T^{\rm in})),\qquad(47)$$

$$\rho_{LL}^{\bar{q}/P}=\frac{1}{2}\int\frac{d^2\boldsymbol{r}_T}{16\pi^3}\int_x^1\frac{dy}{y}\int\frac{\mathrm{d}^2\mathbf{\Delta}_T}{(2\pi)^2}e^{-i\mathbf{\Delta}_T\cdot\boldsymbol{b}_T}\mathrm{sign}(\lambda_{\bar{q}})\sum_{\{\lambda\}}(\psi^{+\star}_{\lambda_B\lambda_q\lambda_{\bar{q}}}(x^{\rm out},y^{\rm out},\boldsymbol{k}_T^{\rm out},\boldsymbol{r}_T^{\rm out})\psi^{+}_{\lambda_B\lambda_q\lambda_{\bar{q}}}(x^{\rm in},y^{\rm in},\boldsymbol{k}_T^{\rm in},\boldsymbol{r}_T^{\rm in}) -\psi^{-\star}_{\lambda_B\lambda_q\lambda_{\bar{q}}}(x^{\rm out},y^{\rm out},\boldsymbol{k}_T^{\rm out},\boldsymbol{r}_T^{\rm out})\psi^{-}_{\lambda_B\lambda_q\lambda_{\bar{q}}}(x^{\rm in},y^{\rm in},\boldsymbol{k}_T^{\rm in},\boldsymbol{r}_T^{\rm in})).\qquad(48)$$

Substituting the LCWFs of the proton into Eqs. (45), (46), (47), and (48), we obtain the expressions for the Wigner distributions in our model as follows:

$$\rho_{UU}^{\bar{q}/P}(x,\boldsymbol{b}_T,\boldsymbol{k}_T) = \frac{g_1^2 g_2^2}{(2\pi)^5}\int_x^1 \frac{dy}{y}\int d^2\boldsymbol{r}_T \int d^2\boldsymbol{\Delta}_T e^{-i\boldsymbol{\Delta}_T\cdot\boldsymbol{b}_T} \times \frac{y(1-y)^2(1-\frac{x}{y})^2[\boldsymbol{r}_T^2 - \frac{1}{4}(1-y)^2\boldsymbol{\Delta}_T^2 + [M_B-(1-y)M]^2][(\boldsymbol{k}_T-\frac{x}{y}\boldsymbol{r}_T)^2 - \frac{1}{4}(1-\frac{x}{y})^2\boldsymbol{\Delta}_T^2 + m^2]}{D_1(y,\boldsymbol{r}_T,\boldsymbol{\Delta}_T)D_2(\frac{x}{y},\boldsymbol{k}_T-\frac{x}{y}\boldsymbol{r}_T,\boldsymbol{\Delta}_T)}, \tag{49}$$

$$\rho_{LU}^{\bar{q}/P}(x,\boldsymbol{b}_T,\boldsymbol{k}_T) = \frac{ig_1^2 g_2^2}{(2\pi)^5}\int_x^1 \frac{dy}{y}\int d^2\boldsymbol{r}_T \int d^2\boldsymbol{\Delta}_T e^{-i\boldsymbol{\Delta}_T\cdot\boldsymbol{b}_T} \frac{y(1-y)^3(1-\frac{x}{y})^2[(\boldsymbol{k}_T-\frac{x}{y}\boldsymbol{r}_T)^2 - \frac{1}{4}(1-\frac{x}{y})^2\boldsymbol{\Delta}_T^2 + m^2]\cdot \boldsymbol{r}_T\times\boldsymbol{\Delta}_T}{D_1(y,\boldsymbol{r}_T,\boldsymbol{\Delta}_T)D_2(\frac{x}{y},\boldsymbol{k}_T-\frac{x}{y}\boldsymbol{r}_T,\boldsymbol{\Delta}_T)}, \tag{50}$$

$$\rho_{UL}^{\bar{q}/P}(x,\boldsymbol{b}_T,\boldsymbol{k}_T) = \frac{ig_1^2 g_2^2}{(2\pi)^5}\int_x^1 \frac{dy}{y}\int d^2\boldsymbol{r}_T \int d^2\boldsymbol{\Delta}_T e^{-i\boldsymbol{\Delta}_T\cdot\boldsymbol{b}_T} \times \frac{y(1-y)^2(1-\frac{x}{y})^3[\boldsymbol{r}_T^2 - \frac{1}{4}(1-y)^2\boldsymbol{\Delta}_T^2 + [M_B-(1-y)M]^2]\cdot(\boldsymbol{k}_T-\frac{x}{y}\boldsymbol{r}_T)\times\boldsymbol{\Delta}_T}{D_1(y,\boldsymbol{r}_T,\boldsymbol{\Delta}_T)D_2(\frac{x}{y},\boldsymbol{k}_T-\frac{x}{y}\boldsymbol{r}_T,\boldsymbol{\Delta}_T)}, \tag{51}$$

$$\rho_{LL}^{\bar{q}/P}(x,\boldsymbol{b}_T,\boldsymbol{k}_T) = -\frac{g_1^2 g_2^2}{(2\pi)^5}\int_x^1 \frac{dy}{y}\int d^2\boldsymbol{r}_T \int d^2\boldsymbol{\Delta}_T e^{-i\boldsymbol{\Delta}_T\cdot\boldsymbol{b}_T} \frac{y(1-y)^3(1-\frac{x}{y})^2\cdot \boldsymbol{r}_T\times\boldsymbol{\Delta}_T\cdot(\boldsymbol{k}_T-\frac{x}{y}\boldsymbol{r}_T)\times\boldsymbol{\Delta}_T}{D_1(y,\boldsymbol{r}_T,\boldsymbol{\Delta}_T)D_2(\frac{x}{y},\boldsymbol{k}_T-\frac{x}{y}\boldsymbol{r}_T,\boldsymbol{\Delta}_T)}. \tag{52}$$

As shown in the above four equations, the contributions to the sea-quark Wigner distributions contains two parts. One is the distribution of the antiquark in the pion meson, the other is distribution of the pion meson in the proton. To quantitatively demonstrate this connection, we also calculate the Wigner distributions $\rho_{UU}^{\pi/P}$, $\rho_{LU}^{\pi/P}$, $\rho_{UU}^{\bar{q}/\pi}$, and $\rho_{UL}^{\bar{q}/\pi}$, which have the following expressions:

$$\begin{aligned}\rho_{UU}^{\pi/P}(y,\boldsymbol{r}_T,b_T) &= \frac{1}{2}\int\frac{\mathrm{d}^2\boldsymbol{\Delta}_T}{(2\pi)^2}e^{-i\boldsymbol{\Delta}_T\cdot\boldsymbol{b}_T}\sum_{\lambda_B}(\psi_{\lambda_B}^{+\star}(y^{\mathrm{out}},\boldsymbol{r}_T^{\mathrm{out}})\psi_{\lambda_B}^{+}(y^{\mathrm{in}},\boldsymbol{r}_T^{\mathrm{in}}) + \psi_{\lambda_B}^{-\star}(y^{\mathrm{out}},\boldsymbol{r}_T^{\mathrm{out}})\psi_{\lambda_B}^{-}(y^{\mathrm{in}},\boldsymbol{r}_T^{\mathrm{in}}))\\ &= \frac{g_1^2}{(2\pi)^2}\int d^2\boldsymbol{\Delta}_T e^{-i\boldsymbol{\Delta}_T\cdot\boldsymbol{b}_T}\frac{y(1-y)^2[\boldsymbol{r}_T^2-\frac{1}{4}(1-y)^2\boldsymbol{\Delta}_T^2+[M_B-(1-y)M]^2]}{D_1(y,\boldsymbol{r}_T,\boldsymbol{\Delta}_T)},\end{aligned} \tag{53}$$

$$\begin{aligned}\rho_{LU}^{\pi/P}(y,\boldsymbol{r}_T,b_T) &= \frac{1}{2}\int\frac{\mathrm{d}^2\boldsymbol{\Delta}_T}{(2\pi)^2}e^{-i\boldsymbol{\Delta}_T\cdot\boldsymbol{b}_T}\sum_{\lambda_B}(\psi_{\lambda_B}^{+\star}(y^{\mathrm{out}},\boldsymbol{r}_T^{\mathrm{out}})\psi_{\lambda_B}^{+}(y^{\mathrm{in}},\boldsymbol{r}_T^{\mathrm{in}}) - \psi_{\lambda_B}^{-\star}(y^{\mathrm{out}},\boldsymbol{r}_T^{\mathrm{out}})\psi_{\lambda_B}^{-}(y^{\mathrm{in}},\boldsymbol{r}_T^{\mathrm{in}}))\\ &= \frac{ig_1^2}{(2\pi)^2}\int d^2\boldsymbol{\Delta}_T e^{-i\boldsymbol{\Delta}_T\cdot\boldsymbol{b}_T}\frac{y(1-y)^3\cdot\boldsymbol{r}_T\times\boldsymbol{\Delta}_T}{D_1(y,\boldsymbol{r}_T,\boldsymbol{\Delta}_T)},\end{aligned} \tag{54}$$

$$\begin{aligned}\rho_{UU}^{\bar{q}/\pi}\left(\frac{x}{y},\boldsymbol{k}_T-\frac{x}{y}\boldsymbol{r}_T,b_T\right) &= \frac{1}{2}\int\frac{\mathrm{d}^2\boldsymbol{\Delta}_T}{(2\pi)^2}e^{-i\boldsymbol{\Delta}_T\cdot\boldsymbol{b}_T}\sum_{\lambda_q,\lambda_{\bar{q}}}\psi_{\lambda_q,\lambda_{\bar{q}}}^{\star}(x^{\mathrm{in}},y^{\mathrm{in}},\boldsymbol{k}_T^{\mathrm{in}},\boldsymbol{r}_T^{\mathrm{in}})\psi_{\lambda_q,\lambda_{\bar{q}}}(x^{\mathrm{out}},y^{\mathrm{out}},\boldsymbol{k}_T^{\mathrm{out}},\boldsymbol{r}_T^{\mathrm{out}})\\ &= \frac{g_2^2}{(2\pi)^2}\int d^2\boldsymbol{\Delta}_T e^{-i\boldsymbol{\Delta}_T\cdot\boldsymbol{b}_T}\frac{(1-\frac{x}{y})^2[(\boldsymbol{k}_T-\frac{x}{y}\boldsymbol{r}_T)^2-\frac{1}{4}(1-\frac{x}{y})^2\boldsymbol{\Delta}_T^2+m^2]}{D_2(\frac{x}{y},\boldsymbol{k}_T-\frac{x}{y}\boldsymbol{r}_T,\boldsymbol{\Delta}_T)},\end{aligned} \tag{55}$$

$$\begin{aligned}\rho_{UL}^{\bar{q}/\pi}\left(\frac{x}{y},\boldsymbol{k}_T-\frac{x}{y}\boldsymbol{r}_T,b_T\right) &= \frac{1}{2}\int\frac{\mathrm{d}^2\boldsymbol{\Delta}_T}{(2\pi)^2}e^{-i\boldsymbol{\Delta}_T\cdot\boldsymbol{b}_T}\mathrm{sign}(\lambda_{\bar{q}})\sum_{\lambda_q,\lambda_{\bar{q}}}\psi_{\lambda_q,\lambda_{\bar{q}}}^{\star}(x^{\mathrm{in}},y^{\mathrm{in}},\boldsymbol{k}_T^{\mathrm{in}},\boldsymbol{r}_T^{\mathrm{in}})\psi_{\lambda_q,\lambda_{\bar{q}}}(x^{\mathrm{out}},y^{\mathrm{out}},\boldsymbol{k}_T^{\mathrm{out}},\boldsymbol{r}_T^{\mathrm{out}})\\ &= \frac{ig_2^2}{(2\pi)^2}\int d^2\boldsymbol{\Delta}_T e^{-i\boldsymbol{\Delta}_T\cdot\boldsymbol{b}_T}\frac{(1-\frac{x}{y})^3\cdot(\boldsymbol{k}_T-\frac{x}{y}\boldsymbol{r}_T)\times\boldsymbol{\Delta}_T}{D_2(\frac{x}{y},\boldsymbol{k}_T-\frac{x}{y}\boldsymbol{r}_T,\boldsymbol{\Delta}_T)}.\end{aligned} \tag{56}$$

Comparing Eqs. (49), (53), and (55), one can find that $\rho_{UU}^{\bar{u}/P}$ can be approximately viewed as the convolution of $\rho_{UU}^{\pi/P}$ and $\rho_{UU}^{\bar{u}/\pi}$. Similar relations holds for $\rho_{LU}^{\bar{u}/P}$, $\rho_{UL}^{\bar{u}/P}$, and $\rho_{LL}^{\bar{u}/P}$.

TABLE I. Values of the parameters obtained from Ref. [42]. The errors of the parameters are also presented.

Parameters	$\bar{u}$	$\bar{d}$
g_1	9.33 ± 0.217	5.79 ± 0.182
g_2	4.46 ± 0.445	4.46 ± 0.445
Λ_π (GeV)	0.223 ± 0.006	0.223 ± 0.006
$\Lambda_{\bar{q}}$ (GeV)	0.510 ± 0.029	0.510 ± 0.029

IV. NUMERICAL RESULTS FOR SEA-QUARK WIGNER DISTRIBUTIONS

In this section, we present the numerical results for the Wigner distributions of the sea quarks $\bar{u}$ and $\bar{d}$. For the parameters g_1, g_2, $\Lambda_{\bar{q}}$, and Λ_π in our model, we adopt the values from Ref. [42], where g_2 and Λ_π are fixed by adopting the GRV leading-order (LO) parametrization [53] to perform the fit for $f_1^{\bar{u}/\pi^-}$ [or $f_1^{\bar{d}/\pi^+}(x)$]. The MSTW2008 LO parametrization [54] is adopted for $f_1^{\bar{u}/P}$ and $f_1^{\bar{d}/P}$ to obtain the values of the parameters g_1 and $\Lambda_{\bar{q}}$. The error bars correspond to the uncertainties of the parametrization at the 90% confidence level. The best values from the fits as well as the errors of the parameters are shown in Table I.

To visualize contribution of the antiquark distribution inside the pion as well as the pion distribution inside the proton, we numerically calculate the Wigner distributions $\rho_{UU}^{\pi/P}$ $\rho_{LU}^{\pi/P}$, $\rho_{UU}^{\bar{q}/\pi}$, and $\rho_{UL}^{\bar{q}/\pi}$.

In the upper panel of Fig. 1, we plot $\rho_{UU}^{\pi^-/P}(y, b_T)$ and $\rho_{UU}^{\pi^+/P}(y, b_T)$ as function of y at $b_T = 0.5$, 1.0, 2.0 GeV^{-1}, respectively. In the lower panel of Fig. 1, we plot $\rho_{LU}^{\pi^-/P}(y, b_T)$ and $\rho_{LU}^{\pi^+/P}(y, b_T)$ as function of y at different values of b_T. We find that in both the cases of π^- and π^+, the size of $y\rho_{UU}$ and $y\rho_{LU}$ decreases with increasing b_T; and the peak of each distribution move to lower-y regions with the increase of b_T. The signs of the unpolarized Wigner distribution and longitudinal-unpolarized Wigner distribution of π^+ in proton are consistent with the case of π^- in proton. In Fig. 2, we plot $\rho_{UU}^{\bar{q}/\pi}(\frac{x}{y}, b_T)$ and $\rho_{UL}^{\bar{q}/\pi}(\frac{x}{y}, b_T)$ at different values of b_T.

In order to show the x-dependence of the sea quark Wigner distribution in the proton, in the left and right panels of Fig. 3, we plot $\rho_{UU}^{\bar{q}/P}(x, b_T)$, $\rho_{LU}^{\bar{q}/P}(x, b_T)$, $\rho_{UL}^{\bar{q}/P}(x, b_T)$, and $\rho_{LL}^{\bar{q}/P}(x, b_T)$ vs x for $\bar{q} = \bar{u}$ and $\bar{d}$ at $b_T = 0.5$, 1.0, 2.0 GeV^{-1}, respectively. We find that in both the cases of $\bar{u}$ and $\bar{d}$, the $\rho_{UU}^{\bar{q}/P}$ and $\rho_{LL}^{\bar{q}/P}$ are positive in the entire x

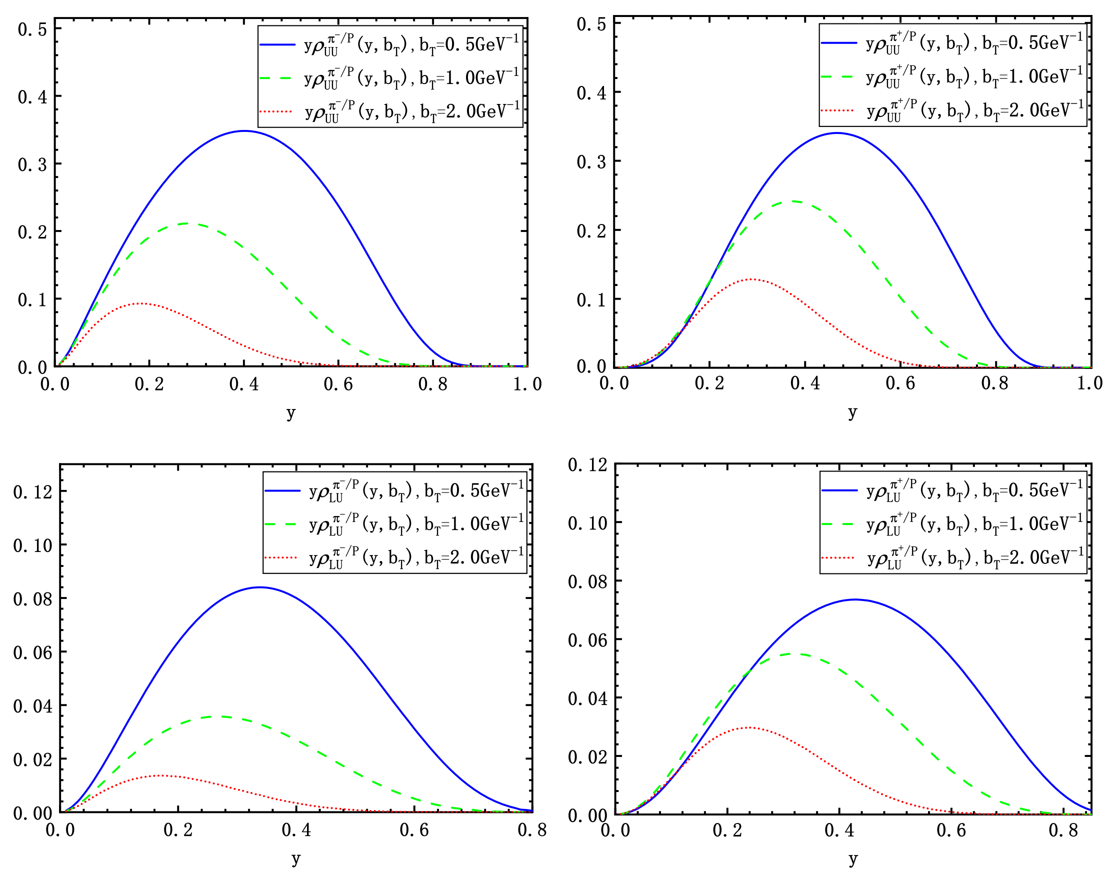

FIG. 1. The Wigner distributions ρ_{UU} (upper panel) and ρ_{LU} (lower panel) of the π^- (left panel) and π^+ (right panel) inside the proton as functions of y at different values of b_T.

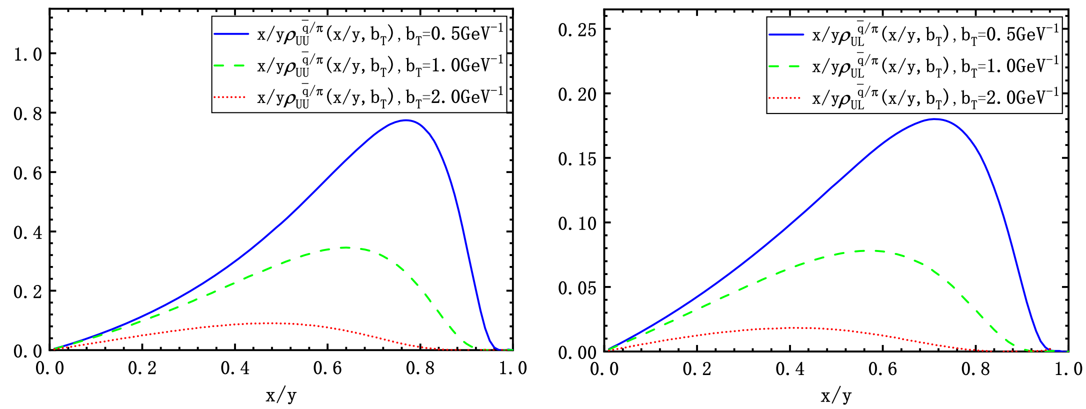

FIG. 2. The Wigner distributions ρ_{UU} (left panel) and ρ_{UL} (right panel) of the $\bar{q}$ inside the π as functions of $\frac{x}{y}$ at different values of b_T.

region, while the signs of $\rho_{LU}^{\bar{q}/P}$ and $\rho_{UL}^{\bar{q}/P}$ are opposite. Moreover, the x-dependence of $x\rho_{UU}^{\bar{q}/P}$, $x\rho_{LU}^{\bar{q}/P}$, $x\rho_{UL}^{\bar{q}/P}$, and $x\rho_{LL}^{\bar{q}/P}$ varies with the change of b_T. To be specific, as b_T increases, the peak of the curves shift from higher x to lower x. In the case of $b_T = 0.5\ \mathrm{GeV}^{-1}$, we also demonstrate the uncertainties band of the Wigner distribution calculated from the errors of the parameters listed in Table I. The numerical result shows that the uncertainty band is around 25% of the distribution.

The Wigner distribution is a five-dimensional function of b_x, b_y, k_x, k_y, x. In the following we study the case of Wigner distributions in the transverse space, namely the transverse-coordinate space (the impact-parameter space) and the transverse-momentum space. The transverse Wigner distributions can be obtained by integrating out the longitudinal momentum fraction x,

$$\rho(\boldsymbol{b}_T, \boldsymbol{k}_T) = \int_0^1 dx \rho(x, \boldsymbol{b}_T, \boldsymbol{k}_T). \tag{57}$$

To extract more information from the Wigner distributions, we also study the mixed transverse Wigner distributions $\rho(b_x, k_y)$, which is a probability density obtained by integrating over b_y and k_x,

$$\rho(b_x, k_y) = \int db_y \int dk_x \rho(\boldsymbol{b}_T, \boldsymbol{k}_T). \tag{58}$$

In Fig. 4, we plot contour plots of the x-integrated Wigner distribution ρ_{UU} of the $\bar{u}$ (left panel) and $\bar{d}$ (right panel) quarks in the proton. The upper panel depicts the distributions in the transverse momentum space with fixed impact parameter $\boldsymbol{b}_T = 0.3\ \mathrm{GeV}^{-1}\ \hat{\boldsymbol{e}}_y$. The central panel depicts the distributions in the impact parameter space with fixed transverse momentum $\boldsymbol{k}_T = 0.3\ \mathrm{GeV}\ \hat{\boldsymbol{e}}_y$. The lower panel depicts the distributions in the mixed plane.

We can observe a left-right symmetry in Fig. 4 which implies that the unpolarized sea quarks in unpolarized proton have no preference for clockwise and anticlockwise motion. Comparing the behaviors of the $\bar{u}$ and $\bar{d}$ quarks, we find that $\rho_{UU}^{\bar{u}/P}$ and $\rho_{UU}^{\bar{d}/P}$ in our model have positive maxima at the center $(k_x = k_y = 0)$, $(b_x = b_y = 0)$, $(b_x = k_y = 0)$, in the transverse momentum plane, transverse coordinate plane and the mixed plane. We also note that the spread behaviors of the distributions for $\bar{u}$ and $\bar{d}$ quarks are similar in $\boldsymbol{k}_T$ and $\boldsymbol{b}_T$ space, that is, the distributions increase faster in x-direction than in y-direction. While we can clearly see that the probability density $\rho_{UU}^{\bar{u}/P}(b_x, k_y)$ and $\rho_{UU}^{\bar{d}/P}(b_x, k_y)$ are extended more in b_x than in k_y.

We also calculate the average quadrupole distortions $Q_b^{ij}(\boldsymbol{k}_T)$ and $Q_k^{ij}(\boldsymbol{b}_T)$ defined as follows:

$$Q_b^{ij}(\boldsymbol{k}_T) = \frac{\int d^2\boldsymbol{b}_T (2b_T^i b_T^j - \delta^{ij}\boldsymbol{b}_T^2)\rho_{UU}(\boldsymbol{b}_T, \boldsymbol{k}_T)}{\int d^2\boldsymbol{b}_T \boldsymbol{b}_T^2 \rho_{UU}(\boldsymbol{b}_T, \boldsymbol{k}_T)},$$

$$Q_k^{ij}(\boldsymbol{b}_T) = \frac{\int d^2\boldsymbol{k}_T (2k_T^i k_T^j - \delta^{ij}\boldsymbol{k}_T^2)\rho_{UU}(\boldsymbol{b}_T, \boldsymbol{k}_T)}{\int d^2\boldsymbol{k}_T \boldsymbol{k}_T^2 \rho_{UU}(\boldsymbol{b}_T, \boldsymbol{k}_T)}. \tag{59}$$

They can be used to quantitatively estimate the distortion of the unpolarized sea quarks in the nucleon. Numerical calculation shows that, at $k_T = 0.3$ GeV, $Q_b(\boldsymbol{k}_T) = 0.442$ for the $\bar{u}$ quark and 0.307 for the $\bar{d}$ quark, respectively. While at $b_T = 0.3\ \mathrm{GeV}^{-1}$, $Q_k(\boldsymbol{b}_T) = -1.535$ for the $\bar{u}$ quark and -1.326 for the $\bar{d}$ quark. Therefore, the distributions $\rho_{UU}^{\bar{u}/P}$ and $\rho_{UU}^{\bar{d}/P}$ in the transverse momentum plane as well as the transverse impact parameter plane have distortions, which indicates the configuration $\boldsymbol{b}_T \perp \boldsymbol{k}_T$ is favored rather than the configuration $\boldsymbol{b}_T \parallel \boldsymbol{k}_T$. These distortions are similar to the valence quark results calculated using the light-cone constituent quark model (LCCQM) [26] and chiral quark soliton model (χQSM) [21]. Our results are different form the results in a light front quark-diquark model where the light-front wave functions are modeled from the soft-wall AdS/QCD prediction. [25].

In Fig. 5, we show the contour plots of the longitudinal-unpolarized Wigner distribution ρ_{LU} for the $\bar{u}$ (left panel) and $\bar{d}$ (right panel) quarks. The upper panel shows the plots

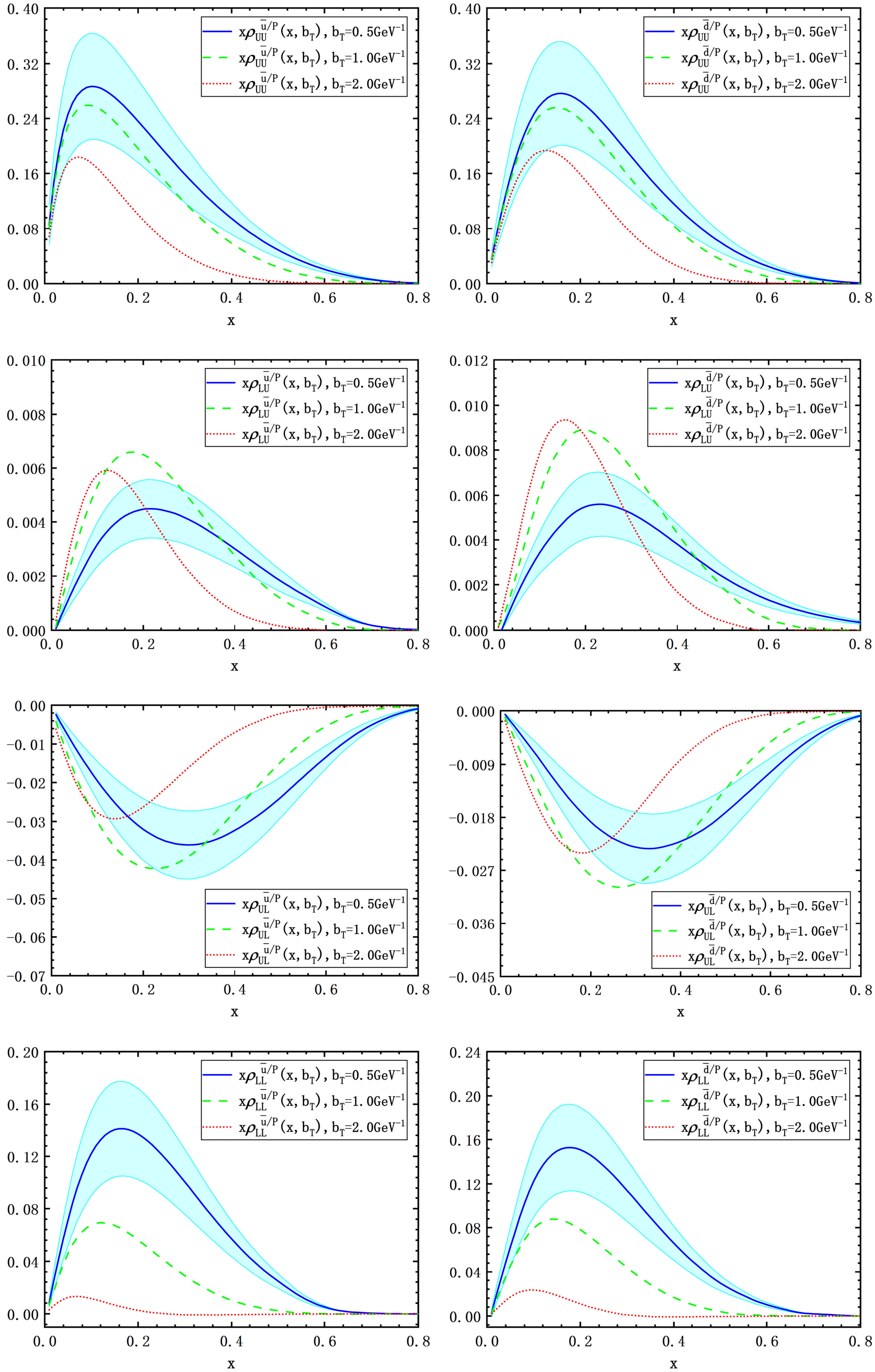

FIG. 3. The Wigner distributions ρ_{UU}, ρ_{LU}, ρ_{UL}, and ρ_{LL} of the $\bar{u}$ (left panel) and $\bar{d}$ (right panel) quarks in the proton as functions of x at different values of b_T. The uncertainty bands of the Wigner distribution at $b_T = 0.5\ \mathrm{GeV}^{-1}$ are also shown.

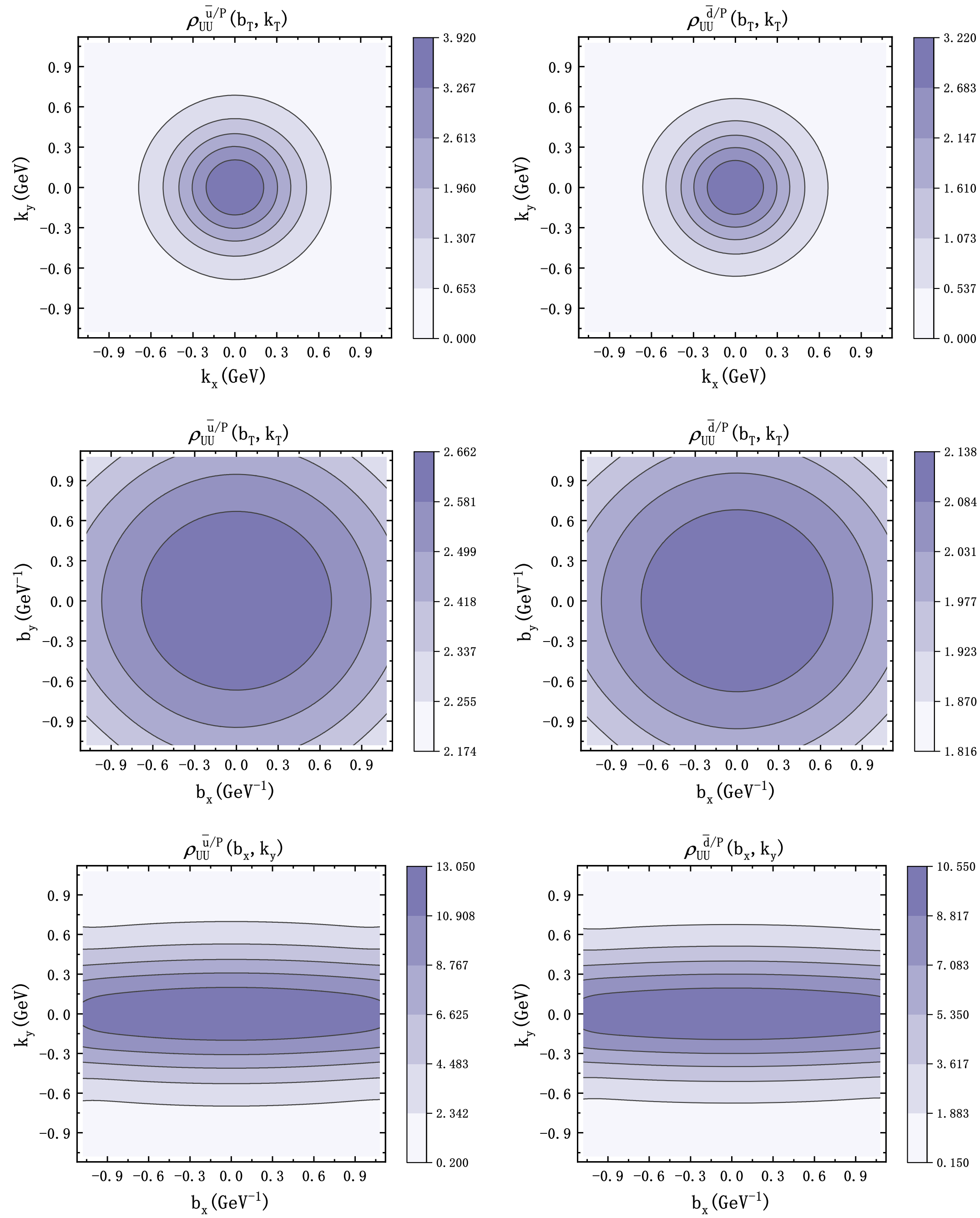

FIG. 4. The Wigner distribution ρ_{UU} of the $\bar{u}$ (left panel) and $\bar{d}$ (right panel) quarks in the proton. The upper panel depicts the distributions in the transverse momentum space with fixed impact parameter $\boldsymbol{b}_T = 0.3\ \mathrm{GeV}^{-1}\ \hat{\boldsymbol{e}}_y$. The central panel depicts the distributions in the impact parameter space with fixed transverse momentum $\boldsymbol{k}_T = 0.3\ \mathrm{GeV}\ \hat{\boldsymbol{e}}_y$. The lower panel depicts the distributions in the mixed plane.

in the $\boldsymbol{k}_T$-space with fixed impact parameter $\boldsymbol{b}_T = 0.3\ \mathrm{GeV}^{-1}\ \hat{\boldsymbol{e}}_y$, the central panel shows the plots in the $\boldsymbol{b}_T$-space with fixed transverse momentum $\boldsymbol{k}_T = 0.3$ GeV $\hat{\boldsymbol{e}}_y$, respectively. There are dipole structures of $\bar{u}$ and $\bar{d}$ quarks in the k_T-space or in the b_T-space. The signs of the polarities for $\rho_{LU}^{\bar{u}/P}$ and $\rho_{LU}^{\bar{d}/P}$ are the same in the k_T-space or in the b_T-space. Particularly, the distributions are positive in $k_x < 0$ region and are negative in $k_x > 0$ region, while they are negative in $b_x < 0$ region and are positive in $b_x > 0$ region. The lower panel shows the mixed Wigner distribution $\rho_{LU}^{\bar{q}/P}(b_x, k_y)$ and depicts a quadrupole structure for both the $\bar{u}$ and $\bar{d}$ quarks. These multipole structures are due to the explicit factor $\epsilon_T^{ij} k_T^i \frac{\partial}{\partial b_T^j}$ in Eq. (18) which breaks the left-right symmetry and implies that the net OAM of the sea

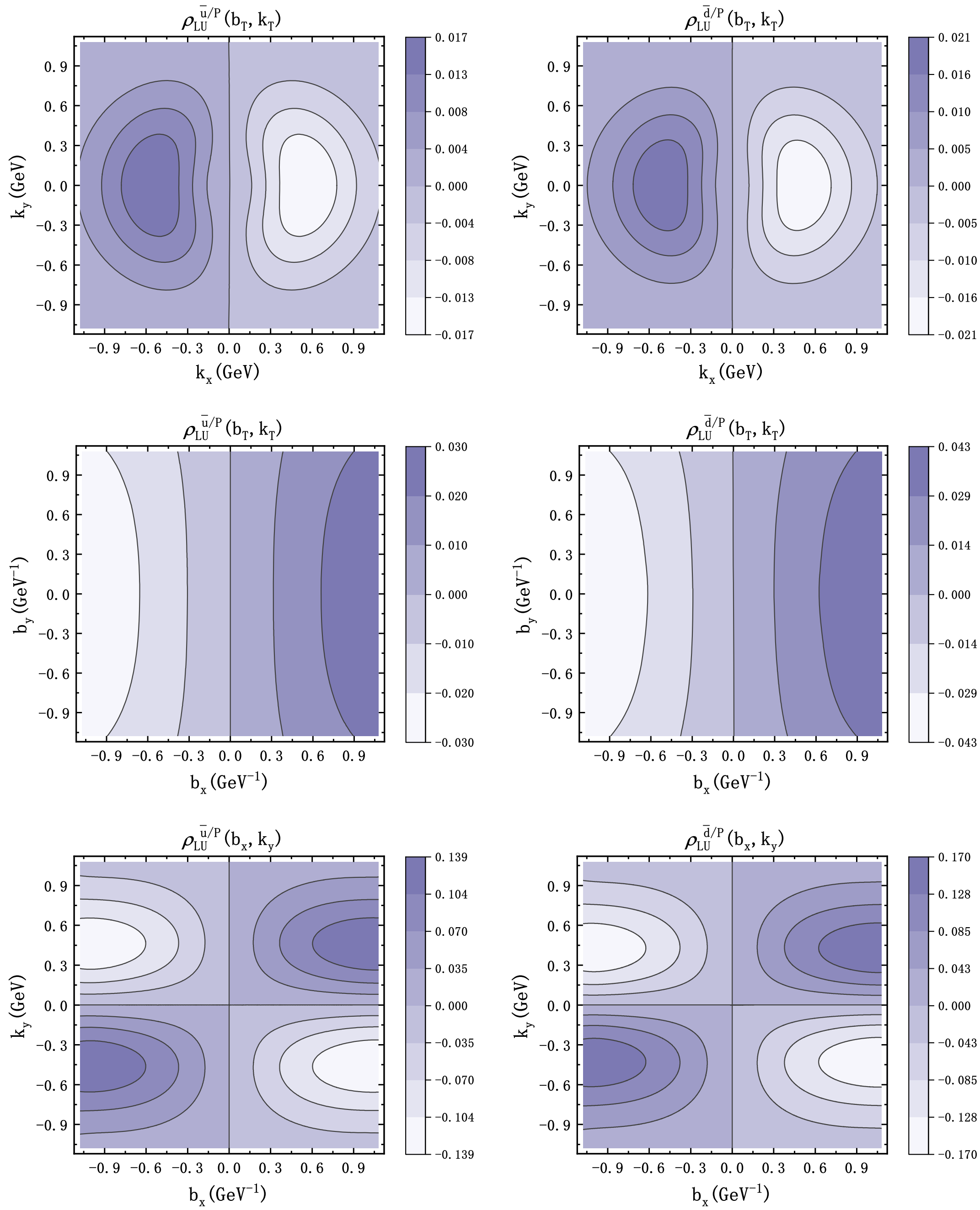

FIG. 5. Similar to Fig. 4, but for the Wigner distribution ρ_{LU} of the $\bar{u}$ (left panel) and $\bar{d}$ (right panel) quarks in the proton.

quark is nonzero. The average sea quark OAM in a proton polarized in the z-direction can be written as

$$\ell_z^{\bar{q}/P} = \int dx d^2\boldsymbol{k}_T d^2\boldsymbol{b}_T (\boldsymbol{b}_T \times \boldsymbol{k}_T)_z \rho^{[\gamma^+]\bar{q}/P}(x, \boldsymbol{b}_T, \boldsymbol{k}_T)$$
$$= \int dx d^2\boldsymbol{k}_T d^2\boldsymbol{b}_T (\boldsymbol{b}_T \times \boldsymbol{k}_T)_z \times [\rho_{UU}^{\bar{q}/P}(x, \boldsymbol{b}_T, \boldsymbol{k}_T) + \rho_{LU}^{\bar{q}/P}(x, \boldsymbol{b}_T, \boldsymbol{k}_T)]. \quad (60)$$

If $\boldsymbol{k}_T$ and $\boldsymbol{b}_T$ are integrated out for $\rho_{UU}^{\bar{q}/P}$, the result is zero, which means that the total angular momentum of constituents sum up to zero in an unpolarized nucleon. Then the sea quark OAM can be written in terms of GTMDs as

$$\ell_z^{\bar{q}/P} = \int dx d^2\boldsymbol{k}_T d^2\boldsymbol{b}_T (\boldsymbol{b}_T \times \boldsymbol{k}_T)_z \rho_{LU}^{\bar{q}/P}(x, \boldsymbol{b}_T, \boldsymbol{k}_T)$$
$$= -\int dx d^2\boldsymbol{k}_T \frac{\boldsymbol{k}_T^2}{M^2} F_{14}^{\bar{q}/P}(x, 0, \boldsymbol{k}_T^2, 0, 0). \quad (61)$$

Numerical calculation yields $\ell_z^{\bar{u}/P} = 0.027$ and $\ell_z^{\bar{d}/P} = 0.051$, which are positive for both the $\bar{u}$ and $\bar{d}$ quarks. This indicates

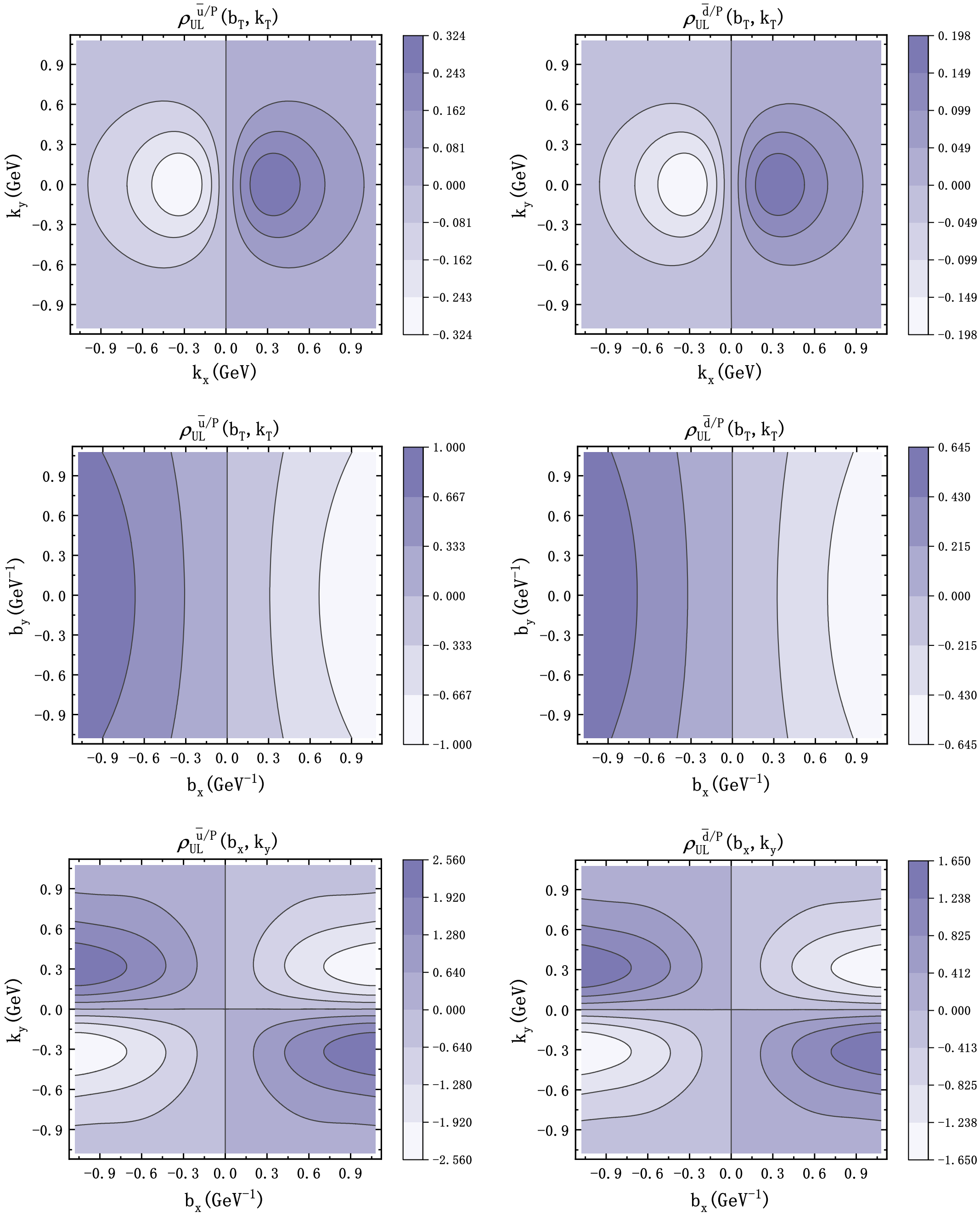

FIG. 6. Similar to Fig. 4, but for the Wigner distribution ρ_{UL} of the $\bar{u}$ (left panel) and $\bar{d}$ (right panel) quarks in the proton.

the sea quark OAM is parallel to the proton spin for both the $\bar{u}$ and $\bar{d}$ quarks in our model.

In Fig. 6 we show the contour plots of the unpolarized-longitudinal Wigner distribution $\rho_{UL}(\boldsymbol{b}_T, \boldsymbol{k}_T)$ and the mixed distributions $\rho_{UL}(b_x, k_y)$ for the $\bar{u}$ (left panel) and $\bar{d}$ (right panel) quarks. Similar to the longitudinal-unpolarized Wigner distribution, $\rho_{UL}(\boldsymbol{b}_T, \boldsymbol{k}_T)$ also has dipolar structures in both the k_T-space and in the b_T-space. However, the sign of ρ_{UL} is opposite to that of ρ_{LU}. In the lower panel, we can observe that the mixed Wigner distribution $\rho_{UL}^{\bar{q}/P}(b_x, k_y)$ has a quadrupole structure. Again, the multipole structure is due to the factor $\epsilon_T^{ij} k_T^i \frac{\partial}{\partial b_T^j}$ in Eq. (19) which essentially reflects quark spin-orbit correlations. The correlation between the longitudinal spin and the OAM of the sea quarks can be defined as

$$C_z^{\bar{q}/P} = \int dx d^2\boldsymbol{k}_T d^2\boldsymbol{b}_T (\boldsymbol{b}_\perp \times \boldsymbol{k}_T)_z \rho_{UL}^{\bar{q}/P}(x, \boldsymbol{k}_T, \boldsymbol{b}_T)$$
$$= \int dx d^2\boldsymbol{k}_T \frac{\boldsymbol{k}_T^2}{M^2} G_{11}^{\bar{q}/P}(x, 0, \boldsymbol{k}_T^2, 0, 0). \quad (62)$$

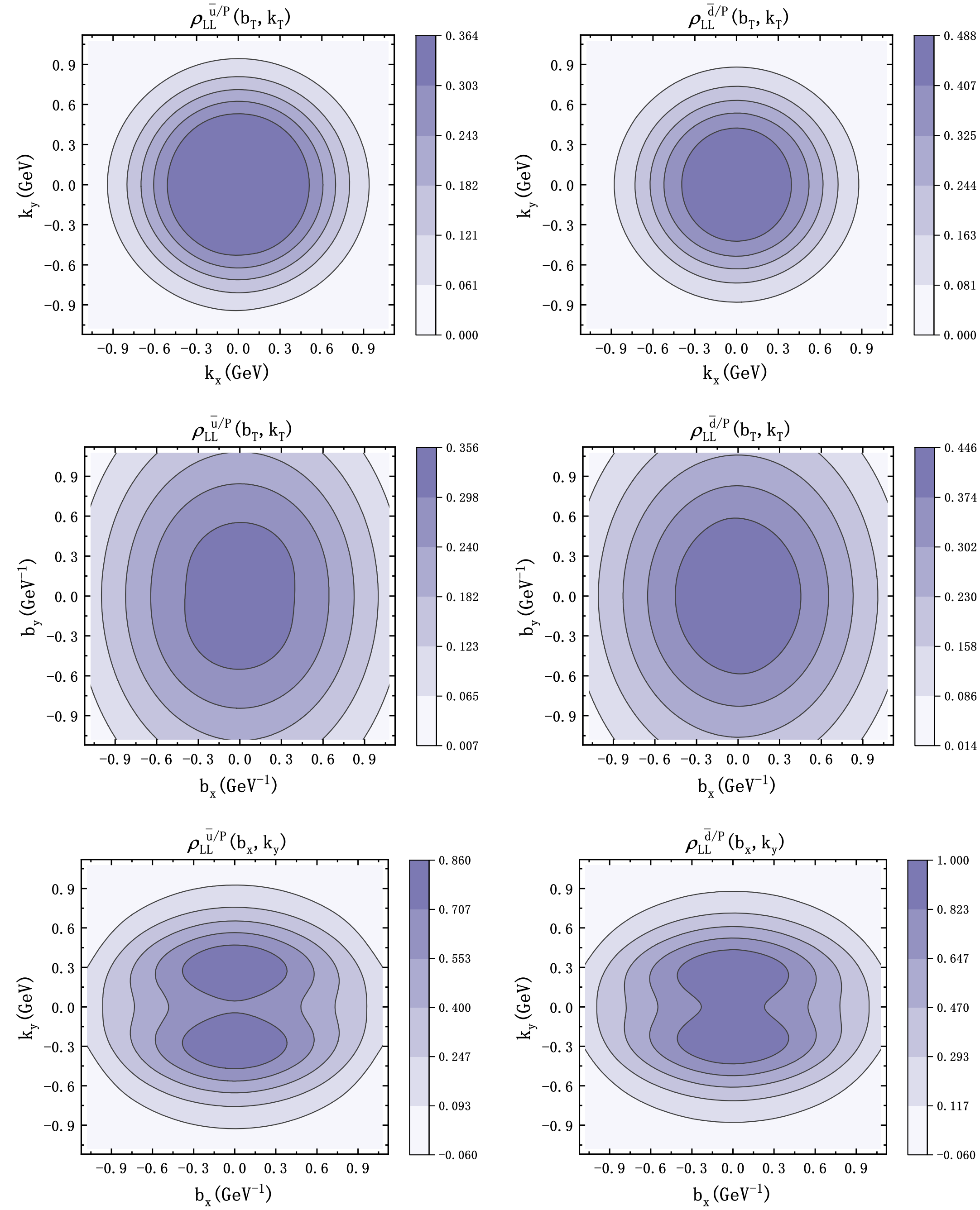

FIG. 7. Similar to Fig. 4, but for the Wigner distribution ρ_{LL} of the $\bar{u}$ (left panel) and $\bar{d}$ (right panel) quarks in the proton.

Numerical calculation shows that both the sea quarks have negative spin-orbit correlation $C_z^{\bar{u}/P} = -0.245$ and $C_z^{\bar{d}/P} = -0.394$, which implies the sea quark spin and OAM tend to be antialigned.

In Fig. 7 we plot the longitudinal-longitudinal Wigner distributions ρ_{LL} for the $\bar{u}$ (left panel) and $\bar{d}$ (right panel) quarks in a way similar to Fig. 4. These distributions describe the phase-space distributions of longitudinal polarized quark in a longitudinal polarized proton, and correspond to the axial charge (Δq) of the nucleon after integrating over transverse variables. We find the distributions of both $\bar{u}$ and $\bar{d}$ quarks are positive, which implies the signs of $\Delta\bar{u}$ and $\Delta\bar{d}$ are positive. For the mixed Wigner distribution, a sign change is observed in large b_x or k_y. This kind of sign change is also found in the longitudinal-longitudinal Wigner distributions of quarks [21,30].

V. CONCLUSION

In this work, we studied the five-dimensional Wigner distributions of sea quarks in the proton using a light-cone model, in which the Wigner distributions and the GTMDs can be expressed as the overlap of LCWFs. To generate the sea quark degree of freedom, we treated the Fock state of proton as a composite system formed by a pion meson and a baryon, where the pion meson is composed in terms of $q\bar{q}$. We numerically calculated the four Wigner distributions ρ_{UU}, ρ_{LU}, ρ_{UL}, and ρ_{LL} of the $\bar{u}$ and $\bar{d}$ quarks in the transverse momentum space and the transverse position space within the overlap representation. Distortions can be found in the distributions ρ_{LU} and ρ_{UL} of the $\bar{u}$ and $\bar{d}$ quarks. Particularly, the dipole structures have been observed in $\rho_{LU}(\boldsymbol{b}_T, \boldsymbol{k}_T)$ and $\rho_{UL}(\boldsymbol{b}_T, \boldsymbol{k}_T)$; and the quadrupole structures have been observed in the mixing distributions $\rho_{LU}(\boldsymbol{b}_x, \boldsymbol{k}_y)$ and $\rho_{UL}(\boldsymbol{b}_x, \boldsymbol{k}_y)$. The polarities of the multipole structures in ρ_{LU} are opposite to those in the ρ_{UL}. The result of the averaged quadrupole distortions $Q_b^{ij}(\boldsymbol{k}_T)$ and $Q_k^{ij}(\boldsymbol{b}_T)$ indicates that the configuration $\boldsymbol{b}_T \perp \boldsymbol{k}_T$ is favored rather than $\boldsymbol{b}_T \parallel \boldsymbol{k}_T$, which is similar to the results for the valence quarks calculated from the light-cone constituent quark model and chiral quark soliton model. We also evaluated the spin-orbit correlation C_z and the OAM of the $\bar{u}$ and $\bar{d}$ quarks using the relation between Wigner distributions and GTMDs. The study on sea-quark Wigner distributions may provide useful information about the sea quarks in proton as well as improve our understanding on the multidimensional image of the proton in the quantum phase space.

ACKNOWLEDGMENTS

This work is partially supported by the National Natural Science Foundation of China under Grant No. 12150013.

[1] R. P. Feynman, Phys. Rev. Lett. **23**, 1415 (1969).
[2] A. Kotzinian, Nucl. Phys. **B441**, 234 (1995).
[3] P. J. Mulders and R. D. Tangerman, Nucl. Phys. **B461**, 197 (1996); **B484**, 538(E) (1997).
[4] D. Boer and P. J. Mulders, Phys. Rev. D **57**, 5780 (1998).
[5] K. Goeke, A. Metz, and M. Schlegel, Phys. Lett. B **618**, 90 (2005).
[6] A. Bacchetta, M. Diehl, K. Goeke, A. Metz, P. J. Mulders, and M. Schlegel, J. High Energy Phys. 02 (2007) 093.
[7] D. Müller, D. Robaschik, B. Geyer, F. M. Dittes, and J. Hořejši, Fortschr. Phys. **42**, 101 (1994).
[8] X. D. Ji, Phys. Rev. D **55**, 7114 (1997).
[9] A. V. Radyushkin, Phys. Rev. D **56**, 5524 (1997).
[10] D. Mueller, D. Robaschik, B. Geyer, F. M. Dittes, and J. Horejsi, Fortschr. Phys. **42**, 101 (1994).
[11] K. Goeke, M. V. Polyakov, and M. Vanderhaeghen, Prog. Part. Nucl. Phys. **47**, 401 (2001).
[12] M. Diehl, Phys. Rep. **388**, 41 (2003).
[13] X. Ji, Annu. Rev. Nucl. Part. Sci. **54**, 413 (2004).
[14] A. V. Belitsky and A. V. Radyushkin, Phys. Rep. **418**, 1 (2005).
[15] S. Boffi and B. Pasquini, Riv. Nuovo Cimento **30**, 387 (2007).
[16] M. Burkardt, Phys. Rev. D **62**, 071503 (2000); **66**, 119903 (E) (2002).
[17] M. Burkardt, Int. J. Mod. Phys. A **18**, 173 (2003).
[18] M. Diehl, Eur. Phys. J. C **25**, 223 (2002); **31**, 277(E) (2003).
[19] X. d. Ji, Phys. Rev. Lett. **91**, 062001 (2003).
[20] A. V. Belitsky, X. d. Ji, and F. Yuan, Phys. Rev. D **69**, 074014 (2004).
[21] C. Lorce and B. Pasquini, Phys. Rev. D **84**, 014015 (2011).
[22] S. Meissner, A. Metz, M. Schlegel, and K. Goeke, J. High Energy Phys. 08 (2008) 038.
[23] S. Meissner, A. Metz, and M. Schlegel, J. High Energy Phys. 08 (2009) 056.
[24] D. Chakrabarti, T. Maji, C. Mondal, and A. Mukherjee, Eur. Phys. J. C **76**, 409 (2016).
[25] D. Chakrabarti, T. Maji, C. Mondal, and A. Mukherjee, Phys. Rev. D **95**, 074028 (2017).
[26] C. Lorce, B. Pasquini, X. Xiong, and F. Yuan, Phys. Rev. D **85**, 114006 (2012).
[27] A. Mukherjee, S. Nair, and V. K. Ojha, Phys. Rev. D **90**, 014024 (2014).
[28] J. More, A. Mukherjee, and S. Nair, Phys. Rev. D **95**, 074039 (2017).
[29] T. Liu, arXiv:1406.7709.
[30] T. Liu and B. Q. Ma, Phys. Rev. D **91**, 034019 (2015).
[31] G. A. Miller, Phys. Rev. D **90**, 113001 (2014).
[32] D. Müller and D. S. Hwang, arXiv:1407.1655.
[33] Y. Hagiwara and Y. Hatta, Nucl. Phys. **A940**, 158 (2015).
[34] Z. L. Ma and Z. Lu, Phys. Rev. D **98**, 054024 (2018).
[35] N. Kaur and H. Dahiya, Eur. Phys. J. A **56**, 172 (2020).
[36] A. Mukkherjee, S. Nair, and V.K. Ojha, Proc. Sci. QCDEV2015 (**2015**) 013.
[37] J. More, A. Mukherjee, and S. Nair, Eur. Phys. J. C **78**, 389 (2018); Y. Hagiwara, Y. Hatta, and T. Ueda, Phys. Rev. D **94**, 094036 (2016).
[38] Y. Hagiwara, Y. Hatta, and T. Ueda, Phys. Rev. D **94**, 094036 (2016).
[39] J. More, A. Mukherjee, and S. Nair, Proc. Sci., DIS2017 (**2018**) 224.
[40] S. J. Brodsky, H. C. Pauli, and S. S. Pinsky, Phys. Rep. **301**, 299 (1998).
[41] S. J. Brodsky and B. Q. Ma, Phys. Lett. B **381**, 317 (1996).
[42] X. Luan and Z. Lu, Phys. Lett. B **833**, 137299 (2022).
[43] A. Rajan, M. Engelhardt, and S. Liuti, Phys. Rev. D **98**, 074022 (2018).
[44] G. P. Lepage and S. J. Brodsky, Phys. Rev. D **22**, 2157 (1980).
[45] S. J. Brodsky, D. S. Hwang, B. Q. Ma, and I. Schmidt, Nucl. Phys. **B593**, 311 (2001).

[46] B. W. Xiao and B. Q. Ma, Phys. Rev. D **68**, 034020 (2003).
[47] A. Bacchetta, F. Conti, and M. Radici, Phys. Rev. D **78**, 074010 (2008).
[48] Z. Lu and I. Schmidt, Phys. Rev. D **75**, 073008 (2007).
[49] S. J. Brodsky, M. Diehl, and D. S. Hwang, Nucl. Phys. **B596**, 99 (2001).
[50] M. Burkardt and D. S. Hwang, Phys. Rev. D **69**, 074032 (2004).
[51] X. Luan and Z. Lu, Eur. Phys. J. C **83**, 504 (2023).
[52] S. Kaur and H. Dahiya, AIP Conf. Proc. **2249**, 030043 (2020).
[53] M. Gluck, E. Reya, and A. Vogt, Z. Phys. C **53**, 651 (1992).
[54] A. D. Martin, W. J. Stirling, R. S. Thorne, and G. Watt, Eur. Phys. J. C **63**, 189 (2009).